TRPM7 facilitates cholinergic vesicle fusion with the plasma membrane

Sebastian Brauchi*, Grigory Krapivinsky, Luba Krapivinsky, and David E. Clapham†

Department of Cardiology, Howard Hughes Medical Institute, Children's Hospital Boston, and Department of Neurobiology, Harvard Medical School, Enders Building 1309, 320 Longwood Avenue, Boston, MA 02115

Contributed by David E. Clapham, January 29, 2008 (sent for review December 3, 2007)

TRPM7, of the transient receptor potential (TRP) family, is both an ion channel and a kinase. Previously, we showed that TRPM7 is located in the membranes of acetylcholine (ACh)-secreting synaptic vesicles of sympathetic neurons, forms a molecular complex with proteins of the vesicular fusion machinery, and is critical for stimulated neurotransmitter release. Here, we targeted pHluorin to small synaptic-like vesicles (SSLV) in PC12 cells and demonstrate that it can serve as a single-vesicle plasma membrane fusion reporter. In PC12 cells, as in sympathetic neurons, TRPM7 is located in ACh-secreting SSLVs. TRPM7 knockdown by siRNA, or abolishing channel activity by expression of a dominant negative TRPM7 pore mutant, decreased the frequency of spontaneous and voltage-stimulated SSLV fusion events without affecting large dense core vesicle secretion. We conclude that the conductance of TRPM7 across the vesicle membrane is important in SSLV fusion.

acetylcholine | PC12 | pHluorin | transient receptor potential channels | single-vesicle fusion

Synaptic vesicles mediate the release of neurotransmitters into the intercellular cleft in response to an action potential. After releasing their contents, synaptic vesicles are taken up, refilled, stored, and reused in a new cycle (1, 2). Synaptic vesicle fusion and recycling is a highly orchestrated process regulated by many proteins (2). Ion channels have been proposed to function in synaptic vesicle membranes (e.g., refs. 3–5), but evidence for their role in successful fusion is lacking.

The process of synaptic vesicle fusion has been studied extensively for >50 years, with much of this work focused on central nervous system (CNS) synaptic vesicles. Studies of secretory vesicles suggests that several themes in CNS synaptic vesicular trafficking and fusion are likely to be common to other types of vesicular trafficking. These include the participation of protein families of the SNARE apparatus in vesicle approximation and initiation of fusion, the targeting roles of small G proteins, and the presence of transporters that accumulate vesicular cargo. Much less well understood are the fusion pore, cargoes destined for insertion into the plasma membrane, and vesicular membrane elements that control vesicle size, tonicity, and voltage.

During our studies of most of the 28 mammalian transient receptor potential (TRP) channel proteins, we found that several family members are commonly localized to vesicles of different sizes but also can function in the plasma membrane. These include TRPC5 (6), TRPV5 (7), TRPM7 (8, 9), and TRPML1 and TRPML3 (10). As with any vesicular membrane protein that incorporates into the plasma membrane, the question arises as to whether the protein also had some functional role in the vesicle in which it had been transported, which seems a particularly important question for TRP ion channels because their mechanisms of activation in native cells generally are not known, and many are increased in the plasma membrane in response to a triggering event (11).

TRPM7 belongs to the TRP ion channel family; conducts monovalent cations, Ca^{2+}, and Mg^{2+}; and is ubiquitously expressed (11, 12). The TRPM7 C terminus is enzymatically active and structurally homologous to other protein kinases except for the inclusion of a zinc-finger domain (13). This kinase phosphorylates TRPM7 (14) and other substrates [e.g., annexin 1 (15) and myosin heavy chain (16)], but its physiological role is not known. The pore of TRPM7 was proposed to be a major entry mechanism for Mg^{2+} ions and, in this role, critical for cell survival (17). TRPM7 is localized in the membrane of sympathetic neuronal acetylcholine (ACh)-secreting synaptic vesicles as part of a molecular complex of synaptic vesicle-specific proteins and its permeability is critical for sympathetic neurotransmitter release (9). Down-regulation of the TRPM7 channel conductance (using siRNA or dominant negative form of the channel) resulted in the attenuation of the neurotransmitter quantal size and probability of neurotransmitter release in response to neuronal stimulation (9). This last observation, relying on measurement of excitatory postsynaptic potential/stimulation coupling, suggested that TRPM7 conductance might affect synaptic vesicle fusion with the plasma membrane. Rat pheochromocytoma PC12 cells have been used to study regulation of neurotransmitter release (18–21). These cells synthesize and store dopamine (DA) in large dense-core vesicles (LDCV) and ACh in small synaptic-like vesicles (SSLV) and release these neurotransmitters by Ca^{2+}-dependent exocytosis (22). Morphologically and biochemically, SSLVs are closely related to neuronal ACh vesicles (23, 24).

The pH-sensitive GFP variant, pHluorin (25) targeted to a lumen of secreted vesicles often has been used as a reporter of synaptic function and vesicular fusion (26–29), including single-vesicle fusion events (30–33). We targeted pHluorin to the acidic lumen of ACh-secreting synaptic vesicles by using the vesicular ACh transporter (VAChT), which is expressed exclusively in synaptic vesicles containing ACh (24, 34). Here, we show that endogenous TRPM7 and expressed VAChT-pHluorin were localized to ACh-secreting SSLVs but not to the monoamine-secreting LDCVs in PC12 cells. VAChT-pHluorin-transfected cells exhibited spontaneous and transient flashes of fluorescence, reflecting single-vesicle fusion events. The frequency of these events was increased by cell depolarization. TRPM7 knockdown by the siRNA, or abolishing channel activity by expression of the dominant negative TRPM7 (dnTRPM7) pore mutant, prevented spontaneous and voltage-stimulated vesicle

Author contributions: S.B. and G.K. contributed equally to this work. S.B., G.K., and D.E.C. designed research; S.B., G.K., and L.K. performed research; S.B., G.K., and L.K. contributed new reagents/analytic tools; S.B., G.K., and D.E.C. analyzed data; and S.B., G.K., and D.E.C. wrote the paper.

The authors declare no conflict of interest.

Freely available online through the PNAS open access option.

*Present address: Laboratorio de Fisiologia Sensorial, 407-D, Instituto de Fisiologia, Facultad de Medicina, Universidad Austral de Chile, Campus Isla Teja, Valdivia, 511-0566, Chile.

†To whom correspondence should be addressed. E-mail: dclapham@enders.tch.harvard.edu.

This article contains supporting information online at www.pnas.org/cgi/content/full/0800881105/DC1.

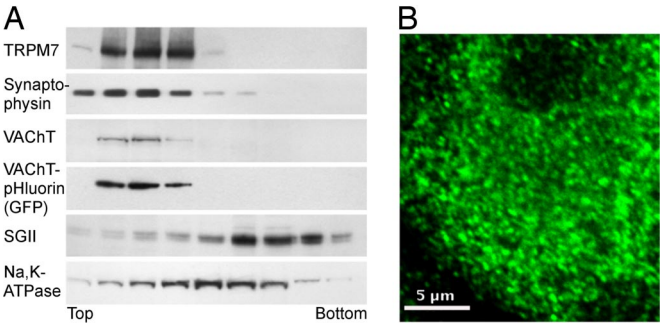

Fig. 1. Endogenous TRPM7 in SSLVs in PC12 cells. (*A*) Sucrose gradient distribution of the PC12 postnuclear supernatant membranes. Western blots show the association of TRPM7, synaptophysin, and VAChT (+/− pHluorin tag) with SSLV fractions. Expressed VAChT-pHluorin was detected with GFP antibody. (*B*) Immunofluorescent confocal image of a nontransfected PC12 cell labeled by anti-TRPM7 antibody. TRPM7 is labeled in vesicles packing the cell cytoplasm and is excluded from the nucleus. (Scale bar: 5 μm.)

fusion events. We conclude that the conductance of TRPM7 across the vesicle membrane is required for vesicle fusion.

Results

Localization of TRPM7 in PC12 Cells. Previous experiments demonstrated that TRPM7 localized to the membrane of synaptic vesicles in sympathetic neurons and colocalized with synaptophysin in the neuromuscular junction. By comparison, TRPM7 was not detected in synapses of glutaminergic hippocampal neurons (9). Speculating that TRPM7 might be expressed in synaptic vesicles carrying positively charged cargo, we examined cholinergic vesicles. PC12 cells contain two major types of secretory vesicles, monoamine-secreting LDCVs, and ACh-secreting SSLVs (34). To determine which vesicles contained TRPM7, we fractionated PC12 postnuclear supernatants on a sucrose gradient, where LDCVs and SSLVs are well separated (35). Fig. 1*A* shows that TRPM7 comigrated with synaptophysin and VAChT (markers of SSLVs) but was absent from fractions containing secretogranin II (SGII)-labeled LDCVs. Note that TRPM7 did not comigrate with the plasma membrane marker Na,K-ATPase (Fig. 1*A*), indicating that the majority of cellular TRPM7 was expressed in SSLVs. Confocal imaging of PC12 cells labeled with TRPM7 antibody also demonstrated that TRPM7 is located in small ($\leq$0.25-μm diameter) vesicles or vesicular aggregates (Fig. 1*B*).

Targeting pHluorin to SSLVs. Because TRPM7 localized predominantly to SSLVs, we targeted pHluorin to the membrane of these vesicles using VAChT, an ACh transporter exclusively localized to SSLVs in PC12 cells (35). VAChT is a 12-transmembrane domain protein with six extramembranous loops protruding into the vesicular lumen (36). The C terminus of VAChT is critical for synaptic vesicle targeting (35), but removal of the first two transmembrane domains does not disrupt vesicular targeting (37). Based on these data, we incorporated pHluorin into the putative first intraluminal loop of VAChT. Sucrose density gradient fractionation of the PC12 cells stably transfected with the VAChT-pHluorin construct showed that pHluorin was expressed in SSLVs (Fig. 1*A*). Exposure of VAChT-pHluorin expressing cells to a membrane-permeant buffer (pH 7.4) potently (>10-fold) enhanced pHluorin fluorescence (data not shown), confirming that pHluorin is in a low pH luminal environment.

Vesicular Fusion Events in PC12 Cells Recorded with VAChT-pHluorin. PC12-expressed VAChT-pHluorin appears in the periplasmic membrane space in discrete structures (vesicles) as small as

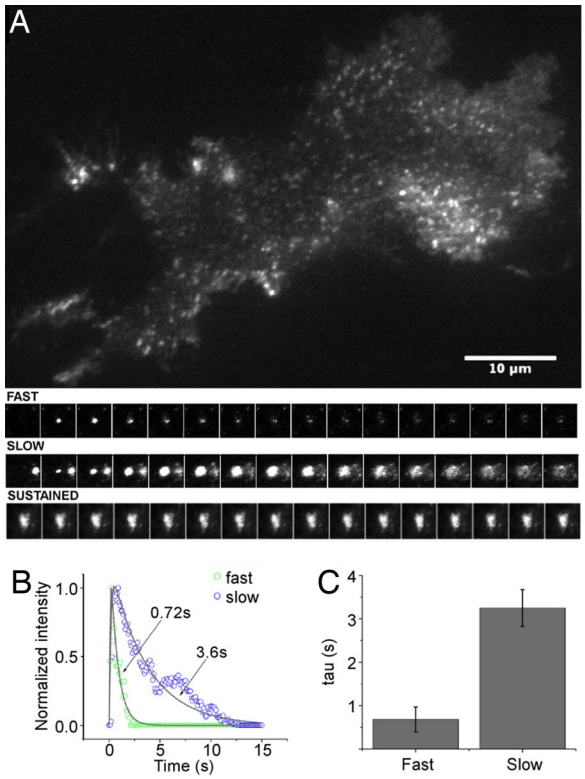

Fig. 2. Cholinergic vesicle fusion in PC12 cells monitored by VAChT-pHluorin fluorescence. (*A*) Single-frame TIRF image of PC12 cell expressing VAChT-pHluorin. (*Insets*) Selected frame sequences from fast, slow, and sustained events. (*B*) Example of fluorescence intensity decay time courses for transient (fast) and full-fusion (slow) events. Solid lines are the single exponential fit of the measured points. (*C*) Bar plot summarizes the kinetics of flash fluorescence decay in VAChT-pHluorin-expressing PC12 cells. The events segregate into fast ($\tau = 0.68 \pm 0.28$ s) and slow ($\tau = 3.25 \pm 0.42$ s) populations. Shown are 54 total events in 20 cells. (Error bars: $\pm$ SEM.)

$\approx$0.25 μm [Fig. 2*A*, supporting information (SI) Movie 1]. Both immobile and mobile vesicles were observed in live cell imaging. Infrequently, bright, discrete, short-lived (<10-s) flashes of fluorescence were observed (Fig. 2*A Insets*, SI Movie 1). These events were interpreted as SSLV fusion to the plasma membrane resulting in exposure of the quenched luminal pHluorin to the more alkaline extracellular media, enhancing pHluorin fluorescence. The fusion kinetics were faster than the 100-ms time resolution of the recordings (Fig. 2*B*, SI Movie 1).

If the flash decay is approximated as a first-order process, three types of events can be distinguished based on the decay kinetics (Fig. 2). We separated these into fast flashes that vanish in <1 s ($\tau = 0.68 \pm 0.28$ s), slowly dissipating flashes ($\tau = 3.25 \pm 0.42$ s), and sustained bright objects (lifetime > 30 s). Fast flash intensities decayed without a change in the size of the object, whereas slowly dissipating flashes diffused into the plane of the membrane (see SI Movie 1). Field stimulation of cells increased the number of flashes, consistent with earlier observations of stimulus-dependent SSLV fusion and ACh release from PC12 cells (23). Similar to a previous study of synaptic vesicle fusion in hippocampal neurons (32), we interpret the fast events as transient vesicle fusion followed by pore closure and vesicle reacidification. Similarly, slowly dissipating flashes represented complete vesicle fusion accompanied by equilibration of vesicle proteins with the cell surface (28). The sustained events were not further analyzed.

TRPM7 Conductance Affects SSLV-Plasma Membrane Fusion. Because TRPM7 localized to the membrane of SSLVs, we next examined

CELL BIOLOGY

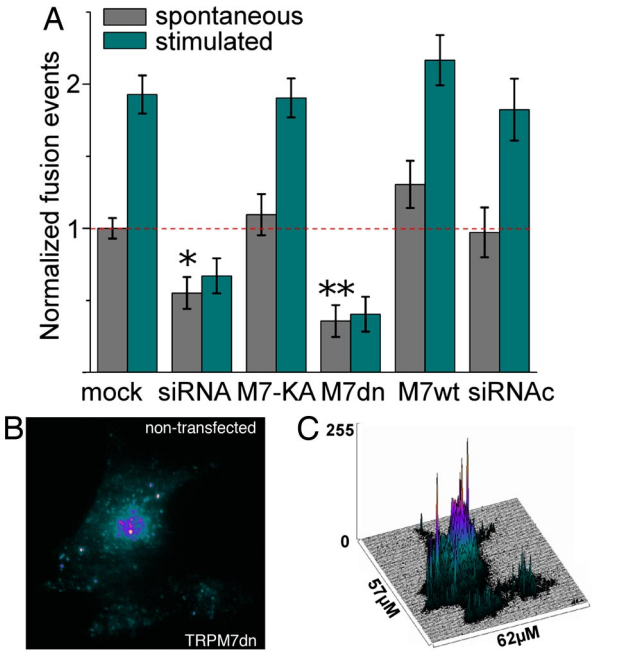

Fig. 3. Reduction in TRPM7 channel activity decreases SSLV fusion event frequency. (*A*) Population analysis of the spontaneous and stimulation-evoked SSLV fusion events with the plasma membrane. For each recorded cell, the total number of fusion events (transient, full, and sustained) in 300 frames was divided by the cell area and normalized to the average accumulated fusion number in vector-transfected cells. TRPM7 knockdown (siRNA; $P < 0.05$; 118 total recorded fusion events, 9 cells) and dnTRPM7 expression (dnM7; $P < 0.001$; 132 total recorded fusion events, 12 cells) substantially reduced fusion frequency. In contrast, overexpression of wt TRPM7 (M7-wt) and kinase-dead TRPM7 (M7-KA) did not alter fusion frequency. Fusion frequency was not significantly different in mock-transfected cells compared with nontransfected cells (data not shown). A total of 56 cells were recorded. (Error bars: ± SEM.) (*B* and *C*) Example illustrating SSLV fusions inhibition with dnTRPM7. (*B*) Simultaneous imaging of nontransfected and dnTRPM7-transfected cells. Image is the sum of 300 background-subtracted frames. (*C*) Three-dimensional projection of intensity (*z*; arbitrary units) and *x*, *y* pixel location of the image in *A*.

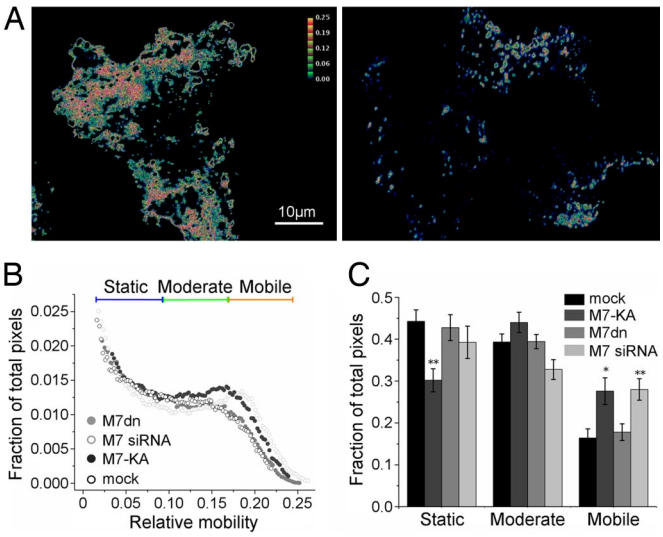

Fig. 4. Increased vesicle mobility in kinase-dead TRPM7-transfected PC12 cells. (*A*) Color-coded mobility images reflect variation of a nonfusing vesicle's position within a 30-s recording (300 frames, see *Materials and Methods*). (*Left*) TRPM7-KA transfected cell. (*Right*) Mock-transfected cell. (*B*) Distribution histogram showing fraction of pixels with the specified mobility. Relative mobility values are defined in the *Materials and Methods*. Bars at top define the regions integrated. (*C*) Population statistics of the integrated relative pixel mobility in TRPM7-transfected PC12 cells. Pixels were separated into three groups (static: $0.01 < \delta < 0.09$; moderately mobile: $0.091 < \delta < 0.17$; and highly mobile: $0.171 < \delta < 0.253$). (Error bars: ± SEM.)

whether TRPM7 affected SSLV fusion with the plasma membrane. Knockdown of TRPM7 protein using siRNA substantially decreased the frequency of SSLV fusion events, whereas transfection with control siRNA had no effect (Fig. 3*A*), indicating that TRPM7 was required for SSLV fusion with the plasma membrane. Similarly, expression of the dnTRPM7 pore mutant dramatically decreased the frequency of the spontaneous fusion events compared with nontransfected or mock-transfected cells (Fig. 3 *A–C*). Population analysis showed that dnTRPM7 expression attenuated SSLV spontaneous fusion frequency by 64% and inhibited field-stimulated fusion frequency by 78% ($P < 0.001$; Fig. 3*A*). These experiments suggest that ion conduction via TRPM7 is critical for SSLV fusion with the plasma membrane.

Overexpression of TRPM7 in PC12 cells did not significantly affect SSLV fusion frequency (Fig. 3*A*). dnTRPM7 or wild-type (wt) channel overexpression did not affect the kinetics of fluorescence decay or the relative percentage of transient and complete fusion events. Could TRPM7 channel activity change intravesicular pH to falsely report or alter the amplitude of fusion events? We compared flash amplitude distributions of cells transfected with different constructs (SI Fig. 5). There were no statistical differences between event amplitudes in mock, dnTRPM7, and TRPM7 siRNA-transfected cells. We conclude that down-regulation of TRPM7 channel activity did not significantly affect intravesicular pH in the time frame of fluorescence reporting.

To test whether the dependence of fusion frequency on TRPM7 was specific to SSLVs, we measured LDCV-mediated norepinephrine release in TRPM7 siRNA-transfected PC12 cells. These measurements demonstrate that TRPM7 knockdown did not affect spontaneous and stimulated LDCV-mediated secretion (SI Fig. 6). We conclude that TRPM7 down-regulation specifically affects SSLV fusion to the plasma membrane.

The Kinase Function of TRPM7 Affects SSLV Mobility. To test whether TRPM7 kinase activity affected SSLV fusion, we overexpressed the TRPM7 kinase-dead mutant (TRPM7-KA) (38, 39). As shown in the Fig. 3*A*, TRPM7-KA expression in PC12 cells did not alter vesicular fusion frequency. However, we noticed that vesicular mobility was higher in TRPM7-KA-transfected cells (SI Movie 2). Calculated diffusion coefficients for wt, dnTRPM7, and TRPM7-KA transfected cells (0.28 ± 0.05, 0.24 ± 0.04, and 0.31 ± 0.02 $\mu m^2 \cdot s^{-1}$, respectively) were not statistically different. To quantify mobility during a 300-frame recording, mobility (*D* values, see *Materials and Methods*) was calculated for each pixel (Fig. 4*A*). Cells expressing the TRPM7-KA mutant contained a significantly larger fraction of the highly mobile SSLVs and a substantially smaller fraction of low-mobility SSLVs (Fig. 4 *B* and *C*). Cells in which endogenous TRPM7 was decreased (siRNA-transfected) also displayed an increased proportion of the highly mobile vesicles. In contrast, no significant change in vesicle mobility was recorded in TRPM7- or dnTRPM7-overexpressing cells (Fig. 4*C*). Thus, inhibition of TRPM7 kinase activity significantly increased the mobility of juxtamembrane SSLVs in PC12 cells.

Discussion

The motivation for this study was to develop a more direct measure of fusion events for TRPM7-containing vesicles. TRPM7 is present in synaptic vesicles of sympathetic neurons and alteration of its function as a channel affects the postsynaptic

response. Detailed analysis of the altered postsynaptic responses suggested that both the size of neurotransmitter quanta and release probability were diminished by TRPM7 knockdown or dnTRPM7 expression (9). Here, we show that TRPM7 is predominantly in SSLVs in PC12, cells and its function is crucial to SSLV fusion to the plasma membrane.

The vesicle luminal pH reporter pHluorin, in combination with total internal reflection fluorescence (TIRF) microscopy, has been extensively validated as a direct assay of acidic vesicle fusion with the membrane (26, 40–42). Fast changes in pHluorin fluorescence is relatively specific for vesicular content exposure to the alkaline extracellular environment. Combining VAChT-tagged pHluorin with TIRF provides a high signal-to-noise ratio because the VAChT reporter is localized strictly to SSLVs, and TIRF narrows detection to within ≈250 nm of the imaged membrane. Using these tools and TRPM7 functional modifications, we found that abrogation of the TRPM7 pore significantly decreased fusion frequency. In contrast, modification of the kinase of TRPM7 did not alter vesicle fusion rates. How might TRPM7 affect vesicle fusion?

Manipulation of TRPM7 channel activity did not affect the relative proportion of transient and complete fusion events (fast, slow, and sustained flashes). TRPM7 down-regulation also did not affect fusion pore closing time or the kinetics of dissipation of the fused vesicle membrane. These data suggest that TRPM7 does not participate in the regulation of the fusion pore itself. Limitations in time resolution did not allow us to evaluate the effect of TRPM7 on pore formation kinetics. Based on these and our previous results (9), we hypothesize that TRPM7 channel conductance is critical to the early steps of vesicle fusion: docking, priming, or pore formation.

When membrane proteins fuse with the plasma membrane, the former vesicular surface faces the extracellular space and the cytoplasmic surfaces remain cytoplasmic. The vesicular membrane itself differs from the plasma membrane; $PI(4,5)P_2$ is excluded from vesicles but abundant in the plasma membrane (43, 44). Two properties of TRPM7 are relevant to these points: (*i*) acid pH potentiates inward divalent conductance (45) and (*ii*) PIP_2 binding activates TRPM7 (46). If TRPM7 gating in vesicles is similar to those on the plasma membrane, TRPM7 should be activated on contact with inner plasmalemmal $PI(4,5)P_2$. In this model, TRPM7 acts as a coincidence detector, opening only when the vesicle pH is low and $PI(4,5)P_2$ in the plasma membrane binds cytoplasmic domains of TRPM7 (e.g., just before fusion). TRPM7 opening at this point would allow ion exchange between the vesicular and cytoplasmic spaces, an event that we speculate is crucial to vesicular fusion.

Finally, we noticed that TRPM7 kinase-dead expression increased vesicle mobility. Multiple experiments have demonstrated that synaptic vesicles and juxtamembrane secretory vesicles are mobile, and that inhibition of protein phosphorylation alters synaptic vesicle mobility (47–51). The possibility that the kinase of TRPM7 phosphorylates synaptic vesicle proteins affecting vesicle behavior warrants further investigation.

Materials and Methods

cDNA Constructs. The rat VAChT coding cDNA sequence was amplified from a rat brain cDNA library and subcloned into EcoRI/XbaI sites of the pcDNA3.1 vector. The coding sequence (minus the stop codon) of ecliptic pHluorin (generously provided by G. Miesenböck, Sloan-Kettering Cancer Center, New York) was amplified by PCR with primers containing PshAI restriction sites and ligated into a unique VAChT PshAI site (base 217 of the coding sequence). N-FLAG-tagged wt mouse TRPM7 (NP_067425), dnTRPM7 (9), and the kinase-dead mutant K1646A (TRPM7-KA) (39) were subcloned into a RpTracer-CAG bicistronic vector. pRTracer-CAG was made from pTracer-CMV2 (Invitogen) by replacing its GFP sequence with mRFP (kindly provided by Roger Tsien, University of California, San Diego) (52). The CMV promoter upstream of the multiple cloning site was replaced by a CAG promoter sequence (53). siRNA was designed to the unique region of rat TRPM7 (732–772 of AF375874; ref. 9). Nonsilencing double-stranded RNA (Ambion) was used as a negative control.

PC12 Cell Fractionation, Western Blotting, and Immunofluorescence. PC12 cell postnuclear supernatants were obtained as described in ref. 35. For equilibrium density fractionation, a postnuclear supernatant (3–5 mg of protein) was loaded onto a continuous 11-ml 0.6–1.6 M (20–46%) sucrose gradient buffered with 20 mM Hepes (pH 7) containing protease inhibitor mixture (Complete, Roche) for sedimentation at 40,000 rpm (SW41 rotor) at 4°C for 3 h. Twelve 1-ml fractions were collected from the bottom of the tube, and 30 μl of each fraction was analyzed by Western blotting with the appropriate antibody (TRPM7 antibodies were described in ref. 9). SGII antibody was provided by R. Fisher-Colbrie (University of Innsbruck, Austria). Commercial antibodies included rabbit Na,K-ATPase (ABR), mouse synaptophysin and FLAG antibodies (Sigma), and goat VAChT antibody (Santa Cruz Biotechnology). For immunofluorescence, cells were fixed with 4% formaldehyde, permeabilized with 0.05% Triton X-100, and immunostained with TRPM7 antibody as described (9, 46). Control experiments with the antibody preabsorbed with antigenic peptide confirmed the specificity of immunostaining. Images were acquired on an Olympus Fluoview-1000 confocal microscope (×60, 1.4 N.A. objective). Basal and Ba^{2+}-stimulated [^{3}H]norepinephrine secretion from PC12 cells was performed as described in ref. 54.

Cell Solutions. PC12 (American Tissue Type Cell Collection) cells were grown on glass coverslips coated with poly(L-lysine) in DMEM/F12 media supplemented with penicillin/streptomycin, 15% horse serum, and 5% fetal bovine serum. PC12 cells stably transfected with the VAChT-pHluorin construct were selected and propagated in the culture media containing 0.4 mg/ml G418. Cells were transfected with Lipofectamine 2000 (Invitrogen) and cultured for 3–5 days. FLAG-TRPM7 protein expression was tested by Western blot and immunofluorescence (FLAG tag). Cells expressing RFP from RpTracer-CAG were selected for imaging.

PC12 cells were imaged in standard external solution consisting of: 140 mM NaCl, 5 mM KCl, 4 mM $CaCl_2$, 2 mM $MgCl_2$, 10 mM glucose, 5 mM EGTA, and 5 mM Na-Hepes (pH 7.4). To increase intravesicular pH, cells were bathed in an external solution in which 50 mM NaCl was replaced by 50 mM NH_4Cl.

TIRF Microscopy. Cells were imaged by using an objective-based TIRF microscope. A 488-nm solid-state diode laser and a 532-nm diode pump laser were focused onto a single-mode optical fiber and transmitted via the rear illumination port of an Olympus IX70 microscope. Digitally synchronized mechanical shutters (Vincent Associates) controlled exposure times. Laser light reflected from a double dichroic mirror (Z488/532RPC; Chroma Tech) passed through a high-numerical aperture objective (×60, N.A. 1.45, oil; Olympus) and was totally internally reflected by the glass–water interface. Fluorescence transmission was passed through an HQ515–30m (Chroma) filter for enhanced GFP, or a D620–60m (Chroma) filter for DsRed2, and collected by a cooled-CCD (ORCA ER II; Hamamatsu). Under our experimental conditions, fluorescent objects were within 250 nm of the glass–water interface (6).

GFP fluorescent images were acquired at 100-ms intervals with MetaMorph software (Universal Imaging). Cells were prebleached (30% laser output power) during a 30- to 40-s period (300 frames) in TIRF mode before the recordings to augment the signal-to-noise ratio. Cells were field-stimulated at 20 Hz with square, 1-ms, 10-V·cm^{-1} voltage pulses across the chamber. Recording under field stimulation always followed an initial 30-s recording of spontaneous activity, and in most cases a third 30-s period of spontaneous activity was recorded after the stimulation period.

Image Analysis. Thirty-second image sequences were analyzed with ImageJ version 1.39c (National Institutes of Health). The background fluorescence was subtracted, and fusion events were identified as changes in intensity above a certain level (at least two times nonfused vesicle average intensity) and counted. The number of events was normalized to cell area. The number of fusions per pixel^2 was normalized by the averaged activity of vector-transfected cells. To calculate fluorescence kinetics, regions of interest (ROIs) were established on previously identified fusion spots, and the fluorescence time course of fusion events was recorded. A single exponential decay function was fitted to the fluorescence relaxation process, and time constants (τ) were calculated. To determine the diffusion constant, we tracked single fluorescent particles (nonfused vesicles) and calculated the mean square displacement (MSD) (55) and the diffusion coefficient ($D = \mathrm{MSD}/4t$).

To quantify vesicle mobility, we consider only the likelihood that a particle moved. The fluorescence signal was filtered to select near-membrane, nonfusing vesicles. The low threshold was set at 2 standard deviations above the mean of the camera and photon noise. The upper threshold was set to remove

transient flashes. Thresholded images were converted into binary format events. For each pixel of the image sequence, the mobility function (δ) was calculated by using the following equation:

$$\delta = \frac{\sum_{1}^{n-1} (f_i - f_{(i+1)})^2}{n},$$

where f is the amplitude value of each pixel (1 or 0) in the binary image, i is a frame number, and n is total number of frames. The processed image reflects object mobility pixel by pixel (''mobility image'') where each pixel represents a color-coded δ value. In mobility distribution histograms, δ values are presented as a fraction of the theoretical maximum (=1). These values were obtained for each cell, normalized, averaged, and presented in probability distribution plots (number of pixels per total pixels).

Data Analysis. ANOVA and Bonferroni tests were used in all cases. We analyzed 9–12 independent experiments and >100 events for every condition. The analysis was performed with GraphPad Prism 5.01 (GraphPad Software). Data plot analysis and curve-fitting were done with Origin 7 (Microcal Corp.). Figures were designed with The GIMP 2.2 (GNU General Public License).

ACKNOWLEDGMENTS. We thank Y. Manasian and S. Gapon for technical assistance and members of the Clapham laboratory for discussion and helpful comments. S.B. was supported by the Pew Program in Biomedical Sciences.

1. Galli T, Haucke V (2001) Cycling of synaptic vesicles: How far? How fast! *Sci STKE* 2001:RE1.
2. Sudhof TC (2004) The synaptic vesicle cycle. *Annu Rev Neurosci* 27:509–547.
3. Rahamimoff R, Fernandez JM (1997) Pre- and postfusion regulation of transmitter release. *Neuron* 18:17–27.
4. Reigada D, *et al*. (2003) Control of neurotransmitter release by an internal gel matrix in synaptic vesicles. *Proc Natl Acad Sci USA* 100:3485–3490.
5. Stanley EF, Ehrenstein G, Russell JT (1988) Evidence for anion channels in secretory vesicles. *Neuroscience* 25:1035–1039.
6. Bezzerides VJ, Ramsey IS, Kotecha S, Greka A, Clapham DE (2004) Rapid vesicular translocation and insertion of TRP channels. *Nat Cell Biol* 6:709–720.
7. Lambers TT, Oancea E, de Groot T, Topala CN, Hoenderop JG, Bindels RJ (2007) Extracellular pH dynamically controls cell surface delivery of functional TRPV5 channels. *Mol Cell Biol* 27:1486–1494.
8. Oancea E, Wolfe JT, Clapham DE (2006) Functional TRPM7 channels accumulate at the plasma membrane in response to fluid flow. *Circ Res* 98:245–253.
9. Krapivinsky G, Mochida S, Krapivinsky L, Cibulsky SM, Clapham DE (2006) The TRPM7 ion channel functions in cholinergic synaptic vesicles and affects transmitter release. *Neuron* 52:485–496.
10. Xu H, Delling M, Li L, Dong X, Clapham DE (2007) Activating mutation in a mucolipin transient receptor potential channel leads to melanocyte loss in varitint waddler mice. *Proc Natl Acad Sci USA* 104:18321–18326.
11. Clapham DE (2003) TRP channels as cellular sensors. *Nature* 426:517–524.
12. Ramsey IS, Delling M, Clapham DE (2006) An introduction to TRP channels. *Annu Rev Physiol* 68:619–647.
13. Yamaguchi H, Matsushita M, Nairn AC, Kuriyan J (2001) Crystal structure of the atypical protein kinase domain of a TRP channel with phosphotransferase activity. *Mol Cell* 7:1047–1057.
14. Runnels LW, Yue L, Clapham DE (2001) TRP-PLIK, a bifunctional protein with kinase and ion channel activities. *Science* 291:1043–1047.
15. Dorovkov MV, Ryazanov AG (2004) Phosphorylation of annexin I by TRPM7 channel-kinase. *J Biol Chem* 279:50643–50646.
16. Clark K, *et al*. (2006) TRPM7, a novel regulator of actomyosin contractility and cell adhesion. *EMBO J* 25:290–301.
17. Schmitz C, *et al*. (2003) Regulation of vertebrate cellular Mg^{2+} homeostasis by TRPM7. *Cell* 114:191–200.
18. Greene LA, Tischler AS (1976) Establishment of a noradrenergic clonal line of rat adrenal pheochromocytoma cells which respond to nerve growth factor. *Proc Natl Acad Sci USA* 73:2424–2428.
19. Sombers LA, Colliver TL, Ewing AG (2002) Differentiated PC12 cells: A better model system for the study of the VMAT's effects on neuronal communication. *Ann NY Acad Sci* 971:86–88.
20. Martin TF, Grishanin RN (2003) PC12 cells as a model for studies of regulated secretion in neuronal and endocrine cells. *Methods Cell Biol* 71:267–286.
21. Eaton MJ, Duplan H (2004) Useful cell lines derived from the adrenal medulla. *Mol Cell Endocrinol* 228:39–52.
22. De Camilli P (1991) Co-secretion of multiple signal molecules from endocrine cells via distinct exocytotic pathways. *Trends Pharmacol Sci* 12:446–448.
23. Greene LA, Rein G (1977) Synthesis, storage and release of acetylcholine by a noradrenergic pheochromocytoma cell line. *Nature* 268:349–351.
24. Weihe E, Tao-Cheng JH, Schafer MK, Erickson JD, Eiden LE (1996) Visualization of the vesicular acetylcholine transporter in cholinergic nerve terminals and its targeting to a specific population of small synaptic vesicles. *Proc Natl Acad Sci USA* 93:3547–3552.
25. Miesenbock G, De Angelis DA, Rothman JE (1998) Visualizing secretion and synaptic transmission with pH-sensitive green fluorescent proteins. *Nature* 394:192–195.
26. Ashby MC, Ibaraki K, Henley JM (2004) It's green outside: Tracking cell surface proteins with pH-sensitive GFP. *Trends Neurosci* 27:257–261.
27. Bozza T, McGann JP, Mombaerts P, Wachowiak M (2004) In vivo imaging of neuronal activity by targeted expression of a genetically encoded probe in the mouse. *Neuron* 42:9–21.
28. Fernandez-Alfonso T, Kwan R, Ryan TA (2006) Synaptic vesicles interchange their membrane proteins with a large surface reservoir during recycling. *Neuron* 51:179–186.
29. Sankaranarayanan S, De Angelis D, Rothman JE, Ryan TA (2000) The use of pHluorins for optical measurements of presynaptic activity. *Biophys J* 79:2199–2208.
30. Balaji J, Ryan TA (2007) Single vesicle imaging reveals that synaptic vesicle exocytosis and endocytosis are coupled by a single stochastic mode. *Proc Natl Acad Sci USA* 51:20576–20581.
31. Bowser DN, Khakh BS (2007) Two forms of single-vesicle astrocyte exocytosis imaged with total internal reflection fluorescence microscopy. *Proc Natl Acad Sci USA* 104:4212–4217.
32. Gandhi SP, Stevens CF (2003) Three modes of synaptic vesicular recycling revealed by single-vesicle imaging. *Nature* 423:607–613.
33. Tsuboi T, Rutter GA (2003) Multiple forms of ''kiss-and-run'' exocytosis revealed by evanescent wave microscopy. *Curr Biol* 13:563–567.
34. Liu Y, Edwards RH (1997) Differential localization of vesicular acetylcholine and monoamine transporters in PC12 cells but not CHO cells. *J Cell Biol* 139:907–916.
35. Varoqui H, Erickson JD (1998) Dissociation of the vesicular acetylcholine transporter domains important for high-affinity transport recognition, binding of vesamicol and targeting to synaptic vesicles. *J Physiol (Paris)* 92:141–144.
36. Eiden LE (1998) The cholinergic gene locus. *J Neurochem* 70:2227–2240.
37. Varoqui H, Erickson JD (1998) The cytoplasmic tail of the vesicular acetylcholine transporter contains a synaptic vesicle targeting signal. *J Biol Chem* 273:9094–9098.
38. Drennan D, Ryazanov AG (2004) Alpha-kinases: Analysis of the family and comparison with conventional protein kinases. *Prog Biophys Mol Biol* 85:1–32.
39. Matsushita M, *et al*. (2005) Channel function is dissociated from the intrinsic kinase activity and autophosphorylation of TRPM7/ChaK1. *J Biol Chem* 280:20793–20803.
40. Yang X, Xu P, Xiao Y, Xiong X, Xu T (2006) Domain requirement for the membrane trafficking and targeting of syntaxin 1A. *J Biol Chem* 281:15457–15463.
41. Becherer U, Pasche M, Nofal S, Hof D, Matti U, Rettig J (2007) Quantifying exocytosis by combination of membrane capacitance measurements and total internal reflection fluorescence microscopy in chromaffin cells. *PLoS One* 2:e505.
42. Prabhat P, *et al*. (2007) Elucidation of intracellular recycling pathways leading to exocytosis of the Fc receptor, FcRn, by using multifocal plane microscopy. *Proc Natl Acad Sci USA* 104:5889–5894.
43. Holz RW, *et al*. (2000) A pleckstrin homology domain specific for phosphatidylinositol 4, 5-bisphosphate (PtdIns-4,5-P2) and fused to green fluorescent protein identifies plasma membrane PtdIns-4,5-P2 as being important in exocytosis. *J Biol Chem* 275:17878–17885.
44. Micheva KD, Holz RW, Smith SJ (2001) Regulation of presynaptic phosphatidylinositol 4,5-biphosphate by neuronal activity. *J Cell Biol* 154:355–368.
45. Jiang J, Li M, Yue L (2005) Potentiation of TRPM7 inward currents by protons. *J Gen Physiol* 126:137–150.
46. Runnels LW, Yue L, Clapham DE (2002) The TRPM7 channel is inactivated by PIP(2) hydrolysis. *Nat Cell Biol* 4:329–336.
47. Betz WJ, Henkel AW (1994) Okadaic acid disrupts clusters of synaptic vesicles in frog motor nerve terminals. *J Cell Biol* 124:843–854.
48. Li Z, Murthy VN (2001) Visualizing postendocytic traffic of synaptic vesicles at hippocampal synapses. *Neuron* 31:593–605.
49. Guatimosim C, Hull C, Von Gersdorff H, Prado MA (2002) Okadaic acid disrupts synaptic vesicle trafficking in a ribbon-type synapse. *J Neurochem* 82:1047–1057.
50. Takahashi M, Itakura M, Kataoka M (2003) New aspects of neurotransmitter release and exocytosis: Regulation of neurotransmitter release by phosphorylation. *J Pharmacol Sci* 93:41–45.
51. Gaffield MA, Rizzoli SO, Betz WJ (2006) Mobility of synaptic vesicles in different pools in resting and stimulated frog motor nerve terminals. *Neuron* 51:317–325.
52. Campbell RE, *et al*. (2002) A monomeric red fluorescent protein. *Proc Natl Acad Sci USA* 99:7877–7882.
53. Niwa H, Yamamura K, Miyazaki J (1991) Efficient selection for high-expression transfectants with a novel eukaryotic vector. *Gene* 108:193–199.
54. Parmer RJ, Mahata M, Mahata S, Sebald MT, O'Connor DT, Miles LA (1997) Tissue plasminogen activator (t-PA) is targeted to the regulated secretory pathway. Catecholamine storage vesicles as a reservoir for the rapid release of t-PA. *J Biol Chem* 272:1976–1982.
55. Qian H, Sheetz MP, Elson EL (1991) Single particle tracking: Analysis of diffusion and flow in two-dimensional systems. *Biophys J* 60:910–921.